Development 137, 1991-1999 (2010) doi:10.1242/dev.045641

Non-molting glossy/shroud encodes a short-chain dehydrogenase/reductase that functions in the 'Black Box' of the ecdysteroid biosynthesis pathway

Ryusuke Niwa[1,2,*,†], Toshiki Namiki[3,*], Katsuhiko Ito[4,*], Yuko Shimada-Niwa[1], Makoto Kiuchi[3], Shinpei Kawaoka[4], Takumi Kayukawa[3], Yutaka Banno[5], Yoshinori Fujimoto[6], Shuji Shigenobu[7], Satoru Kobayashi[7], Toru Shimada[4], Susumu Katsuma[4] and Tetsuro Shinoda[3,†]

SUMMARY

In insects, the precise timing of molting and metamorphosis is strictly guided by a principal steroid hormone, ecdysone. Among the multiple conversion steps for synthesizing ecdysone from dietary cholesterol, the conversion of 7-dehydrocholesterol to 5β-ketodiol, the so-called 'Black Box', is thought to be the important rate-limiting step. Although a number of genes essential for ecdysone synthesis have recently been revealed, much less is known about the genes that are crucial for functioning in the Black Box. Here we report on a novel ecdysteroidgenic gene, *non-molting glossy* (*nm-g*)/*shroud* (*sro*), which encodes a short-chain dehydrogenase/reductase. This gene was first isolated by positional cloning of the *nm-g* mutant of the silkworm *Bombyx mori*, which exhibits a low ecdysteroid titer and consequently causes a larval arrest phenotype. In the fruit fly, *Drosophila melanogaster*, the closest gene to *nm-g* is encoded by the *sro* locus, one of the Halloween mutant members that are characterized by embryonic ecdysone deficiency. The lethality of the *sro* mutant is rescued by the overexpression of either *sro* or *nm-g* genes, indicating that these two genes are orthologous. Both the *nm-g* and the *sro* genes are predominantly expressed in tissues producing ecdysone, such as the prothoracic glands and the ovaries. Furthermore, the phenotypes caused by the loss of function of these genes are restored by the application of ecdysteroids and their precursor 5β-ketodiol, but not by cholesterol or 7-dehydrocholesterol. Altogether, we conclude that the Nm-g/Sro family protein is an essential enzyme for ecdysteroidogenesis working in the Black Box.

KEY WORDS: Black Box, *Bombyx mori*, *Drosophila melanogaster*, Ecdysone, Halloween mutant, Prothoracic gland, Short-chain dehydrogenase/reductase

INTRODUCTION

In insects and other arthropods, steroid hormones designated as ecdysteroids, such as ecdysone and its derivative, 20-hydroxyecdysone (20E), control the precise temporal progression of development (Thummel, 2001; Gilbert et al., 2002; Mirth and Riddiford, 2007; Spindler et al., 2009). Ecdysone is synthesized via a series of hydroxylation and oxidation steps in the prothoracic gland (PG) during postembryonic development and in the ovary in adults (Gilbert et al., 2002). Ecdysone is subsequently converted to 20E by 20-hydroxylase present in the peripheral tissues (Gilbert et al., 2002).

In the past decade, molecular genetic studies using the fruit fly *Drosophila melanogaster* have successfully identified several genes crucial for the conversion of intermediates in ecdysone biosynthesis. The dehydrogenation of cholesterol to 7-dehydrocholesterol (7dC), the first step for synthesizing ecdysone, is mediated by the Rieske-domain protein Neverland (Nvd) (Yoshiyama et al., 2006) (Fig. 1). The terminal hydroxylation steps in ecdysteroid biosynthesis in the PG, namely 5β-ketodiol to ecdysone, are catalyzed by three cytochrome P450 mono-oxygenases: Phantom (Phm; CYP306A1), Disembodied (Dib; CYP302A1) and Shadow (Sad; CYP315A1) (Chávez et al., 2000; Warren et al., 2002; Niwa et al., 2004; Warren et al., 2004; Niwa et al., 2005) (Fig. 1). The conversion of ecdysone to 20E is also mediated by a P450 mono-oxygenase, Shade (Shd; CYP314A1), in the peripheral tissues (Petryk et al., 2003). All of these genes encoding P450 enzymes have been identified from embryonic lethal mutants called Halloween mutants that exhibit ecdysone deficiency in embryos (Chávez et al., 2000; Gilbert and Warren, 2005).

Although the first and final biochemical steps of ecdysteroid biosynthesis are relatively well-characterized at the molecular level, little is known about the enzymes involved in the intervening conversion processes from 7dC to 5β-ketodiol. These uncharacterized reactions are commonly referred to as the 'Black Box' (Fig. 1), for which no stable intermediate has been identified. It is believed that the Black Box contains the rate-limiting step in the production of ecdysone (Warren and Hetru, 1990; Gilbert et al.,

[1]Graduate School of Life and Environmental Sciences, University of Tsukuba, Tennoudai 1-1-1, Tsukuba, Ibaraki 305-8572, Japan. [2]Initiative for the Promotion of Young Scientists' Independent Research, University of Tsukuba, Tennoudai 1-1-1, Tsukuba, Ibaraki 305-8577, Japan. [3]National Institute of Agrobiological Sciences, Owashi 1-2, Tsukuba, Ibaraki 305-8634, Japan. [4]Department of Agricultural and Environmental Biology, Graduate School of Agricultural and Life Sciences, The University of Tokyo, Yayoi 1-1-1, Bunkyo-ku, Tokyo 113-8657, Japan. [5]Institute of Genetic Resources, Faculty of Agriculture, Kyushu University Graduate School, Higashi-ku, Fukuoka 812-8581, Japan. [6]Department of Chemistry and Materials Science, Tokyo Institute of Technology, Meguro, Tokyo 152-8551, Japan. [7]Okazaki Institute for Integrative Bioscience, National Institute for Basic Biology, National Institutes of Natural Sciences, Higashiyama, Myodaiji, Okazaki 444-8787, Japan.

*These authors contributed equally to this work
†Authors for correspondence (ryusuke-niwa@umin.ac.jp; shinoda@affrc.go.jp)

Accepted 7 April 2010

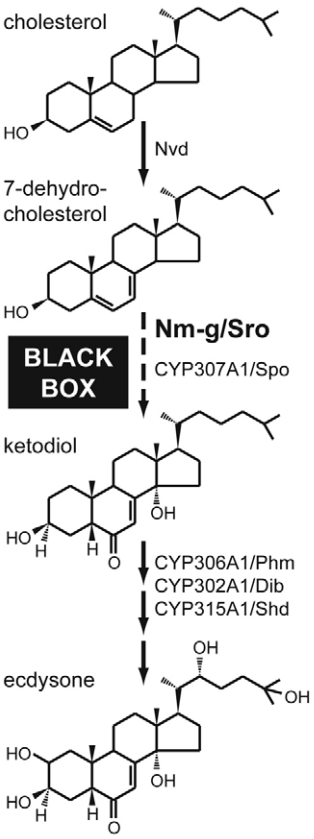

Fig. 1. A schematic representation of the roles of Nm-g/Sro in ecdysteroid biosynthesis. Nm-g/Sro plays a crucial role in the conversion step(s) between 7-dehydrocholesterol and 5β-ketodiol, the so-called Black Box.

2002) and is ultimately under the regulation of the neuropeptide prothoracicotropic hormone (PTTH) and a subsequent intracellular signaling pathway (Gilbert et al., 2002; Rewitz et al., 2009). A recent study reported that the Halloween gene *spook* (*spo*) and its paralog *spookier* (*spok*), which also encode cytochrome P450s, play a role in the Black Box (Namiki et al., 2005; Ono et al., 2006). However, it is unclear whether *spo* and *spok* are only a single genetic component of the Black Box because the conversion of 7dC to 5β-ketodiol must be achieved through modifications at multiple carbon positions. These modifications include the oxidation of 3β-alcohol to its ketone form, the oxidation of carbon-6 with concomitant loss of the 4β- and 6-hydrogens to form the 6-keto group, and 14α-hydroxylation (Warren and Hetru, 1990; Gilbert et al., 2002; Lafont et al., 2005). Therefore, the identification and functional characterization of genes involved in the Black Box are essential to understand the mechanisms by which ecdysteroidogenesis is precisely controlled in insects.

To uncover an unidentified gene responsible for ecdysteroid biosynthesis, we focused on a genetic mutant designated *non-molting glossy* (*nm-g*) of the silkworm *Bombyx mori*, another classical model insect utilized for the study of endocrinology. Previous studies have revealed that the *nm-g* mutant causes a reduced ecdysteroid titer and larval arrest mainly at the first instar stage (Nagata et al., 1987; Tanaka, 1998). Here, we report that the gene responsible for *nm-g* mutants encodes a short-chain dehydrogenase/reductase (SDR). We also show that the *shroud* (*sro*) mutant, one of the Halloween mutants in *D. melanogaster*, is caused through the loss of function of the *nm-g* ortholog. Finally, we demonstrate that the Nm-g/Sro family acts as an indispensable player for a specific conversion step called the Black Box in ecdysteroid biosynthesis (Fig. 1).

MATERIALS AND METHODS

Animal strains and culture

Wild-type strains of the silkworm *B. mori* were C108 (The University of Tokyo) and the KINSHU × SHOWA F_1 hybrid. The *nm-g* mutant strain (Nagata et al., 1987) was a46 (Kyushu University). Silkworm larvae were reared on mulberry leaves or on an artificial diet (Silkmate, Nihon Nosan Kogyo) at 25°C.

D. melanogaster flies were reared on standard agar-cornmeal medium at 25°C under a 12-hour light, 12-hour dark photoperiod. *yw* was used as the wild-type. sro^{1} (Jürgens et al., 1984) was obtained from the *Drosophila* Genetic Resource Center. Other strains were kind gifts as follows: sro^{P54} and $sro^{O4\text{-}105}$ (Giesen et al., 2003) from C. Klämbt (University of Münster, Germany); kay^{1} (Zeitlinger et al., 1997) from D. Bohmann (University of Rochester, NY, USA); *2-286-GAL4*, in which *GAL4* is expressed during embryogenesis (see Fig. S1 in the supplementary material) and strongly expressed in the larval PG (Timmons et al., 1997), from C. S. Thummel (University of Utah, USA); and *ptth* neuron-ablated flies (*ptth-GAL4;UAS-grim*) (McBrayer et al., 2007), *phm-GAL4* and the *TM3[Actin5c-GFP]* balancer from M. B. O'Connor (University of Minnesota, USA). *sro* RNAi was performed using three independent *UAS-sro-inverted repeat* (*IR*) transgenic lines that targeted different *CG12068* (*sro*) open reading frame (ORF) regions (see Fig. S2A in the supplementary material). *UAS-sro-IR1* was established as described below. *UAS-sro-IR2* and *UAS-sro-IR3* were obtained from the Vienna *Drosophila* RNAi Center.

Genetic mapping and molecular cloning of *nm-g*

For linkage and recombination analysis, a single-pair cross between a female (C108) and a male (a46) produced the F_1 offspring. Then, the cross (a46 × C108) × (a46 × C108) produced F_2 progeny. Primer sets were designed from the single nucleotide polymorphism (SNP) linkage map (Yamamoto et al., 2006; Yamamoto et al., 2008) and the *B. mori* genome sequence (Mita et al., 2004; Xia et al., 2008) (see Table S1A in the supplementary material). PCR and SNP markers were generated at each position on linkage group 17 and the markers that showed polymorphisms between C108 and a46 were used for the genetic analysis of 839 F_2 individuals with the *nm-g* phenotype (see Table S2 in the supplementary material). Annotation of candidate genes by KAIKObase and KAIKOblast, genome PCR and reverse transcription (RT)-PCR using cDNA prepared from the whole body of the first instar larvae was performed as previously described (Ito et al., 2008; Ito et al., 2009). The primer sets for the seven *nm-g* candidate genes (Fig. 2B) are listed in Table S1B in the supplementary material. The full-length structure of the *nm-g* gene was determined by sequencing the clone fprWP04_F_D06, which was found in the *B. mori* expressed-sequence tag database (http://silkbase.ab.a.u-tokyo.ac.jp/cgi-bin/index.cgi). Genomic structures around the *nm-g* locus of wild type and the *nm-g* mutant were determined by sequencing genomic fragments amplified with the primers described in Table S1C in the supplementary material (Fig. 2D). The nucleotide sequences of *B. mori nm-g* and *D. melanogaster sro* have been deposited in GenBank (accession numbers AB361434 and AB361435, respectively).

Quantitative RT-PCR (qRT-PCR)

For quantifying the *sro* transcript level in sro^{P54} homozygous and control embryos, individual embryos from sro^{P54}/*TM3[Actin5c-GFP]* parents were collected 2-6 hours after egg laying (AEL). Extraction of both genomic DNA and total RNA from individual embryos was performed as essentially described (Ghanim and White, 2006). sro^{P54} homozygote and other progenies were distinguished by PCR amplification of the *GFP* gene region on the *TM3* balancer with genome DNA and primers (see Table S1D in the supplementary material).Total RNA for each individual genotyped embryo was isolated by RNAiso reagent (TaKaRa). For other experiments, total RNA was isolated using the RNeasy Mini Kit (Qiagen). Synthesis of single-stranded cDNA and qRT-PCR were performed as previously

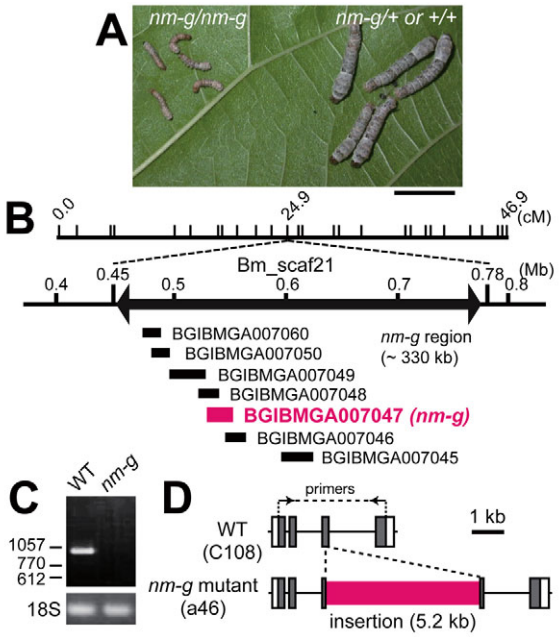

Fig. 2. The identification and characterization of the *B. mori nm-g* locus. (**A**) *nm-g* homozygous mutants (left) and *nm-g* heterozygous or wild-type larvae (right) photographed 10 days after hatching. Scale bar: 1 cm. (**B**) Mapping of *nm-g*. The *nm-g* locus was in an ~330 kb region between 0.45 M and 0.78 M nucleotides on Bm_scaf21, located around 24.9 cM on linkage group 17. The ~330 kb region contains seven putative transcripts predicted by the Chinese genome consortium. The *BGIBMGA007047* (*nm-g*) gene is marked in red. See Fig. S2A-C in the supplementary material for more details. (**C**) RT-PCR analysis with wild type (WT) and *nm-g* mutants using the primers indicated in D. 18S ribosome was used as an internal control. (**D**) The genomic structure of the *nm-g* gene in wild type (C108) and *nm-g* mutant strains (a46). White boxes, gray boxes and black bars indicate untranslated regions, the ORF and intronic regions, respectively. An insertion on the *nm-g* mutant chromosome is marked by red.

described (Shinoda and Itoyama, 2003). Primers for qRT-PCR are listed in Table S1E in the supplementary material. Serial dilutions of a plasmid containing the ORF of each gene were used as standards. The level of each transcript was normalized to *rp49* in the same sample.

UAS vectors, overexpression of genes and generation of transgenic strains

Overexpression of genes in flies was performed using the GAL4/UAS system (Brand and Perrimon, 1993). To generate UAS constructs to overexpress *nm-g* and *sro*, specific primers (see Table S1F in the supplementary material) were used for PCR to add a *Bgl*II site and a *Not*I site to the 5′ and the 3′ ends, respectively, of each of the cDNA fragments corresponding to the ORFs. Each ORF region was digested with *Bgl*II and *Not*I and the fragment was ligated into a pUAST vector. For transgenic RNAi (Kennerdell and Carthew, 2000), we generated a *UAS-sro-IR1* that was a genomic-cDNA fusion construct as represented in Fig. S2B in the supplementary material. The primers for constructing the *UAS-sro-IR1* are described in Table S1G in the supplementary material. The *D. melanogaster* transformants were established using standard protocols.

Identification of point mutations in EMS-induced *sro* mutants

Genomic DNA was extracted from the balanced sro^{1} or $sro^{O4\text{-}105}$ heterozygous adults. DNA fragments covering the entire *sro* gene region and the first exon of *kayak*/*D-fos*/*CG33956* were amplified by PCR using genomic DNA with primers (see Table S1H in the supplementary material) and then sequenced.

In situ RNA hybridization

To generate a template for synthesizing sense and antisense *sro* RNA probes, the ORF region of *sro* was amplified by PCR using primers (see Table S1I in the supplementary material) and subcloned to pGEM-T (Promega). Synthesis of DIG-labeled RNA probes and in situ hybridization were performed as previously described (Niwa et al., 2004).

Rescue experiments with ecdysteroid intermediates

Cholesterol, 7dC, ecdysone and 20E were purchased from Sigma. 5β-ketodiol (3β,14α-dihydroxy-5β-cholest-7-en-6-one) was prepared as previously described (Niwa et al., 2004). For rescue experiments for *D. melanogaster* embryos, $sro^{1}/sro^{O4\text{-}105}$ trans-heterozygous embryos were collected 6-9 hours AEL, dechorionated and incubated with or without 100 mM 20E for 3 hours as previously described (Ono et al., 2006). After incubation, the embryos were washed and allowed to develop further on agar-apple juice plates with yeast paste containing 1 mg/ml or no 20E in 3.3% ethanol at a final concentration. For the feeding rescue experiment for *B. mori nm-g* mutants, we collected the *nm-g* mutant larvae at day 5 of first instar. At this stage, wild-type animals entered into the molting stage, whereas the *nm-g* mutants did not. Because the *nm-g* mutant larvae were smaller than the control larvae, the *nm-g*/*nm-g* homozygotes were distinguished from the $nm\text{-}g/+^{nm\text{-}g}$ and $+^{nm\text{-}g}/+^{nm\text{-}g}$ animals by body size. Ten selected *nm-g* mutant larvae were reared on 100 mg mulberry leaves coated with 100 μl of 0.2 mg/ml of each intermediate dissolved in 100% ethanol. Two days later, developmental stages were scored. The percentage of *nm-g* mutants that entered into the molting stage was calculated. This assay was performed at least five times for each intermediate. To assess the phenotype of *D. melanogaster sro* RNAi animals, the 24-36 hours AEL first instar larvae of *yw;UAS-sro-IR/+;2-286-GAL4/+* were collected. Progeny carrying either *UAS* or *GAL4* transgenes alone were used as controls. Feeding rescue experiments for *D. melanogaster* larvae were performed as previously described (Yoshiyama et al., 2006).

Ecdysteroid titer measurements

Day 5 first instar *nm-g* mutants were transferred to mulberry leaves supplemented with ecdysteroid intermediates. Then, silkworms were collected and squashed 1 day after the transfer, which was 1 day before >90% of animals entered into the molting stage by the feeding of ecdysone or 5β-ketodiol (Table 2). Day 3 wild-type first instar larvae were used as a control (Fig. 7) because this stage was 1 day before the wild-type animals entered into the molting stage under our culture conditions. In experiments using *D. melanogaster*, control and *sro* RNAi larvae were collected 54-66 hours AEL when a large amount of 20E is produced in wild type (Sullivan and Thummel, 2003). Sample preparation and a radioimmunoassay for ecdysteroid titer measurement were performed as described (Takeda et al., 1986; Yoshiyama et al., 2006). 20E was used as the standard.

RESULTS

Positional cloning of *nm-g* in *B. mori*

To specify a candidate region for a responsible gene of *nm-g* mutant (Fig. 2A), we performed genetic linkage analysis using the SNP linkage map and the *B. mori* genome sequence. First, we roughly mapped and narrowed the *nm-g* mutation region on linkage group 17 (Fig. 2B; see also Fig. S3A and Table S2 in the supplementary material). Two scaffolds (Bm_scaf131 and Bm_scaf21) corresponding to this region were found in the *B. mori* genome database (see Fig. S3B in the supplementary material). We then designed primer sets based on the sequences of these scaffolds (see Table S1A in the supplementary material) and further delimited the *nm-g* locus to an ~330 kb-long position on Bm_scaf21 that contained seven predicted genes (Fig. 2B; see Fig. S3C in the supplementary material). RT-PCR experiments revealed that the expression of one of the seven genes, *BGIBMGA007047*, was detected in the wild-type but not in the *nm-g* homozygous larvae (Fig. 2C), whereas the expression of the other genes examined did not exhibit any obvious differences between the

wild-type and the *nm-g* homozygous larvae (see Fig. S3D in the supplementary material). Moreover, the *nm-g* mutant chromosome had a 5.2 kb insertion sequence in the third exon of *BGIBMGA007047* (Fig. 2D; see Fig. S4 in the supplementary material). Because the insertion disrupted the entire *BGIBMGA007047* ORF, we concluded that *BGIBMGA007047* was the gene responsible for *nm-g* mutants ($+^{nm\text{-}g}$). Hereafter, we describe the *BGIBMGA007047* or $+^{nm\text{-}g}$ gene as *nm-g* for simplicity.

The *D. melanogaster* Halloween mutant *shroud* causes loss of function of the *nm-g* ortholog

A BLAST search revealed that the *B. mori nm-g* gene is the most closely related to *CG12068* of all of the predicted genes of *D. melanogaster* (Fig. 3A,B). *CG12068* is located at the 99C1 cytological position on the third chromosome. Curiously, this position is in the vicinity of the Halloween mutant *shroud* (*sro*) that has been mapped to the 99A-100A interval (Jürgens et al., 1984). *sro* is known to exhibit the typical Halloween-class phenotype (Jürgens et al., 1984; Chávez et al., 2000), epitomized by an undifferentiated cuticular structure in embryos (Fig. 4A,B). Conversely, a previous study has reported that *sro* is allelic to the *kayak*/*D-fos*/*CG33956* (*kay*) gene (Giesen et al., 2003), which is indeed located next to *CG12068* on the third chromosome (Fig. 4C). A basis of this conclusion is that two independent EMS-induced lethal alleles of *sro*, sro^{1} and $sro^{O4\text{-}105}$, were not complemented with sro^{P54} (Fig. 4D), in which a P-element is inserted in the 5′ upstream region of *kay* (Giesen et al., 2003) (Fig. 4C). Paradoxically, the strongest *kay* mutation, kay^{1}, results in embryonic lethality but not the typical Halloween-class morphological defects (Jürgens et al., 1984; Zeitlinger et al., 1997; Giesen et al., 2003). We therefore examined whether *CG12068*, but not *kay*, was the true gene responsible for *sro* mutants.

First, the EMS-induced sro^{1} and $sro^{O4\text{-}105}$ alleles were complementary to the kay^{1} allele (Fig. 4D), suggesting that the gene responsible for the EMS-induced *sro* mutants must be different from the *kay* gene. This result was consistent with another recent report (Hudson and Goldstein, 2008). Second, qRT-PCR analysis revealed that the sro^{P54} homozygous mutant embryos exhibited a large reduction in the *CG12068* transcript level compared with the control embryos (Fig. 4E), indicating that sro^{P54} causes loss of function not only in *kay* but also in *CG12068*. Third, both the sro^{1} and the $sro^{O4\text{-}105}$ chromosomes had C-to-T nucleotide substitutions (see Fig. S5 in the supplementary material), which led to nonsense mutations that disrupted the catalytic centers of the deduced CG12068 protein structures (Fig. 3A; see Fig. S5 in the supplementary material). Finally, the lethality of the sro^{1} mutant was rescued by the overexpression of either *D. melanogaster CG12068* or *B. mori nm-g* (Table 1). These results strongly support our hypothesis that *CG12068* is the gene responsible for the *sro* mutants and is the functional ortholog of *nm-g*. Hereafter, we call the *CG12068* gene *sro*.

The embryonic lethality of the *D. melanogaster sro* mutant is rescued by delivering 20E

As the Halloween mutants have defects in ecdysteroid biosynthesis (Chávez et al., 2000), we next determined whether the lethality of the *sro* mutants was rescued by delivering 20E midway through embryogenesis. With control ethanol treatment, no $sro^{1}/sro^{O4\text{-}105}$ embryos (n=134) developed into first instar larvae. By contrast, by the 20E application, approximately 52% of those embryos (n=259) hatched into first instar larvae, whereas the rescued animals died at the first instar larvae on a normal diet (n=59). This larval lethality was also due to ecdysone deficiency, as approximately 45% of the rescued $sro^{1}/sro^{O4\text{-}105}$ first instar larvae (n=58) grew into the second larval stage on a diet supplemented with 20E. These results suggest that the *sro* is required for ecdysone production in both embryonic and larval development in *D. melanogaster*.

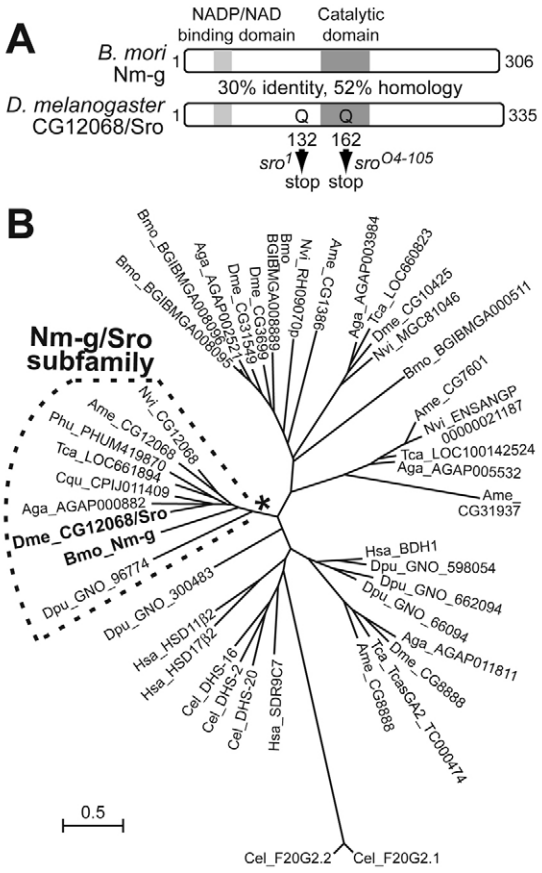

Fig. 3. *nm-g*/*sro* is a conserved short-chain dehydrogenase/reductase (SDR) among insect species. (**A**) Predicted polypeptides from *B. mori BGIBMGA007047* (*nm-g*; AB361434) and its closest gene from *D. melanogaster CG12068* (*sro*; AB361435). See Fig. S4 in the supplementary material for a detailed sequence alignment. Positions of an NAD and/or NADP binding domain (light gray) and a catalytic domain (dark gray) are indicated. Nonsense mutations at positions 132 and 162 of the Sro protein in the sro^{1} and the $sro^{O4\text{-}105}$ mutants, respectively, are also represented. (**B**) A phylogenetic tree showing the relationship of Nm-g and Sro to other close SDR members. The rootless tree was generated based on the entire amino acid sequence by the neighbor-joining method through the ClustalW program (Thompson et al., 1994). Names and GenBank accession numbers of the proteins represented in this tree are listed in Table S4 in the supplementary material. The tree includes the top four or top five BLAST hits closest to *D. melanogaster* Sro from each genome of the following species: *Anopheles gambiae* (Aga), *Apis mellifera* (Ame), *Tribolium castaneum* (Tca), *Nasonia vitripennis* (Nvi), the crustacean *Daphnia pulex* (Dpu), the nematode *Caenorhabditis elegans* (Cel) and the human *Homo sapiens* (Hsa). The *nm-g*/*sro* orthologs are also found in *Culex quinquefasciatus* (Cqu) and *Pediculus humanus corporis* (Phu). A bootstrap value of the branching point of the *nm-g*/*sro* subfamily (asterisk) was 785 per 1000 counts. A scale bar shows the number of amino acid substitutions per site between two sequences.

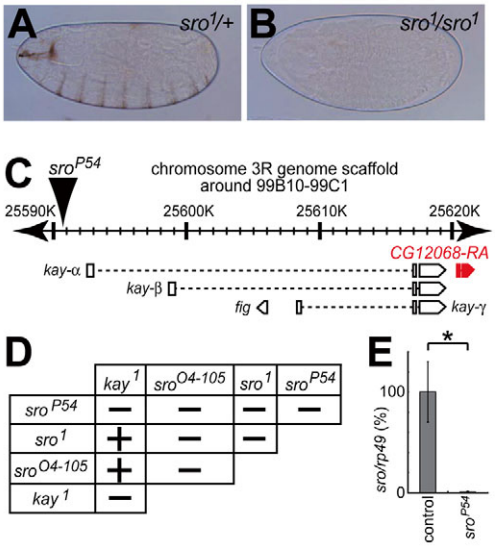

Fig. 4. The characterization of *CG12068* (*sro*) mutants. (**A**,**B**) Embryonic cuticle structures of the *sro*^{1} heterozygote (A) and homozygote (B). (**C**) The genomic and exon-intron structures of *kayak*, *fig* (white boxes) and *CG12068* (red boxes) corresponding to 99B10-99C1 on the chromosome 3R genome scaffold. *kay* splice variants and *fig* have previously been described (Hudson and Goldstein, 2008). The arrowhead indicates the position of the P-element insertion in the *sro*^{P54} allele (Giesen et al., 2003). (**D**) A complementation grid for the pairwise matings of the mutant alleles of *kay* and *sro*. A plus (+) indicates complementation and a minus (–) indicates failure to complement. (**E**) qRT-PCR analysis of *sro* transcripts normalized to internal *rp49* levels 2-6 hours AEL from individual control embryos (*sro*^{P54}*/TM3[Actin5c-GFP]* and *TM3[Actin5c-GFP]/TM3[Actin5c-GFP]*; *n*=25) and *sro*^{P54} homozygotes (*n*=30). Each error bar represents standard error of the mean (s.e.m.). *, *P*<0.05 by Student's *t*-test.

nm-g/sro encode a short-chain dehydrogenase/reductase

The predicted full ORF of *B. mori nm-g*/*D. melanogaster sro* encodes a protein that belongs to short-chain dehydrogenase/reductases (SDRs), which constitute a large family of enzymes that catalyze NAD(P)(H)-dependent oxidation and/or reduction reactions (Kallberg et al., 2002; Kavanagh et al., 2008). The primary structure of Nm-g/Sro contains several motifs that are typical of SDR proteins, such as a NAD/NADP binding domain, a catalytic center (Fig. 3A; see Fig. S5 in the supplementary material) and other characteristic secondary structures (see Fig. S5 in the supplementary material). A phylogenetic analysis demonstrates that putative *nm-g*/*sro* orthologs are conserved among insect species as well as the crustacean *Daphnia pulex* (Fig. 3B). Whereas the Nm-g/Sro proteins are substantially similar to some vertebrate steroidogenic SDR proteins, such as 11β- and 17β-hydroxysteroid dehydrogenases (Wu et al., 2007) (Fig. 3B; see Fig. S5 in the supplementary material), apparent *nm-g*/*sro* orthologs cannot be found outside the arthropods (Fig. 3B). These results suggest that the occurrence of *nm-g*/*sro* genes is limited to animals that produce ecdysteroids, similar to the Halloween P450 genes (Rewitz and Gilbert, 2008).

Table 1. *sro*^{1} lethality was rescued by *sro*/*nm-g* overexpression

Genotype	Number of adults
+/+; 2-286-GAL4 sro^{1}*/+ sro*^{1}	0 (308)
UAS-sro/+; sro^{1}*/sro*^{1}	0 (170)
UAS-nm-g/+; sro^{1}*/sro*^{1}	0 (138)
UAS-sro/+; 2-286-GAL4 sro^{1}*/+ sro*^{1}	128 (286)
UAS-nm-g/+; 2-286-GAL4 sro^{1}*/+ sro*^{1}	57 (270)

The numbers of viable adults were scored. Parentheses indicate the number of viable progeny with the presence of balancer markers from the parental strains.

nm-g/sro is predominantly expressed in the PG and ovaries

Spatial expression of *nm-g* was restricted to the PG and was weak in the ovary, both of which synthesize ecdysone (Fig. 5A). A change in the *nm-g* expression level in the PG also correlated well with the change in the hemolymph ecdysteroid titer during development (Fig. 5B), which was similar to other ecdysteroidogenic genes, such as *B. mori spo* and *phm* (see Fig. S6 in the supplementary material).

In *D. melanogaster*, the early embryonic expression of the Halloween P450 genes is essential for embryonic ecdysteroid production prior to the formation of the PG (Gilbert and Warren, 2005; Namiki et al., 2005; Ono et al., 2006). The embryonic expression pattern of *sro* also correlated with a change in the embryonic ecdysteroid titer in *D. melanogaster*. Although no or little *sro* mRNA was maternally loaded (Fig. 5C; see Fig. S7A in the supplementary material), the *sro* transcript level drastically increased around stage 3, mainly in the epithelial cells (see Fig. S7B in the supplementary material). The maximal level of embryonic *sro* expression was observed at 2-4 hours AEL (Fig. 5C), which roughly corresponds to embryonic stages 5-9 (see Fig. S7C-E in the supplementary material). Then, *sro* expression was gradually decreased in later embryogenesis (Fig. 5C; see Fig. S7F,G in the supplementary material). These results suggest that *sro* mRNA accumulates prior to the maximal ecdysteroid titer during *D. melanogaster* embryogenesis (Maróy et al., 1988).

During the larval stage, *sro* was expressed predominantly in the ring gland, which contains the PG cells of the first instar larval stage and later stages (Fig. 5D,E; see Fig. S7I in the supplementary material). In the ring gland, the *sro* transcript was exclusively observed in the PG (Fig. 5F) but not in the corpus allatum or corpus cardiacum, which are components of the ring gland (Fig. 5F). In the developing egg chambers of adult females, *sro* was expressed in the nurse cells (Fig. 5G; see Fig. S7H in the supplementary material), in which some genes involved in ecdysone production are known to be expressed (see Discussion). Furthermore, similar to the *nvd* and Halloween P450 genes (McBrayer et al., 2007), *sro* expression was significantly reduced in the third instar larvae in which the *ptth* gene-expressing neurons were ablated (Fig. 5H). All of these results demonstrate that *D. melanogaster sro* expression is also spatiotemporally correlated with ecdysone production.

The larval arrest phenotype of the loss of *nm-g/sro* function is rescued by feeding of 20E in both *B. mori* and *D. melanogaster*

To assess the importance of *sro* in the PG during *D. melanogaster* larval development, we also examined the phenotypes of either the overexpression or the knockdown of the *sro* gene in the PG of developing flies using the GAL4/UAS system. In a wild-type background, the overexpression of *sro* using the PG-expressing *GAL4* lines *2-286-GAL4* and *phm-GAL4* had no visible effect on development (data not shown). To knock down *sro*, we performed transgenic RNA interference (RNAi) experiments (Kennerdell and

Carthew, 2000) using a transgenic line carrying an inverted repeat construct corresponding to the *sro* mRNA under the control of the *UAS* promoter (*UAS-sro-IR1*; see Fig. S2A,B in the supplementary material). Hereafter, we refer to the animals in which the *sro* RNAi was driven by *2-286-GAL4* and *UAS-sro-IR1* as '*sro* RNAi animals' for simplicity. In the *sro* RNAi animals, an ~90% reduction in the level of the *sro* mRNA was achieved at the first and second instar larvae (see Fig. S2C,D in the supplementary material). *sro* RNAi animals completed embryogenesis, hatched normally and showed no apparent morphological or behavioral defects until the second instar larvae. After 72 hours AEL, the control animals possessed large mouth hooks with numerous small teeth and everted anterior spiracular papillae of the trachea, which is typical for third instar larvae. However, even after 72 hours AEL, *sro* RNAi animals retained the second instar larva-type morphologies for both the mouth hook and the anterior spiracular insertion (Fig. 6A,C). All *sro* RNAi animals died prior to 144 hours AEL at the second instar larval stage. The identical larval arrest phenotype was also observed when using the *sro* RNAi driven by the other PG-expressing *GAL4* driver, *phm-GAL4*. In addition, two other *sro* RNAi transgenic lines that targeted different regions of the *sro* gene (see Fig. S2A in the supplementary material) also caused lethality when driven by *2-286-GAL4* or *phm-GAL4* (see Table S3 in the supplementary material), suggesting that the effect of the RNAi was specific to *sro* and was not an off-target effect.

We also found that *sro* RNAi animals fed yeast paste containing 20E just after hatching grew to the third instar larval stage, as judged by the mouth hook and anterior spiracular morphologies (Table 2; Fig. 6B,D). Similarly, consistently with a previous report (Nagata et al., 1987; Tanaka, 1998), the larval arrest phenotype of the *B. mori nm-g* mutant was rescued by feeding the larvae ecdysone (Table 2; see Fig. S8 in the supplementary material). These results demonstrate that *nm-g* and *sro* are essential for larval development via the regulation of ecdysone production.

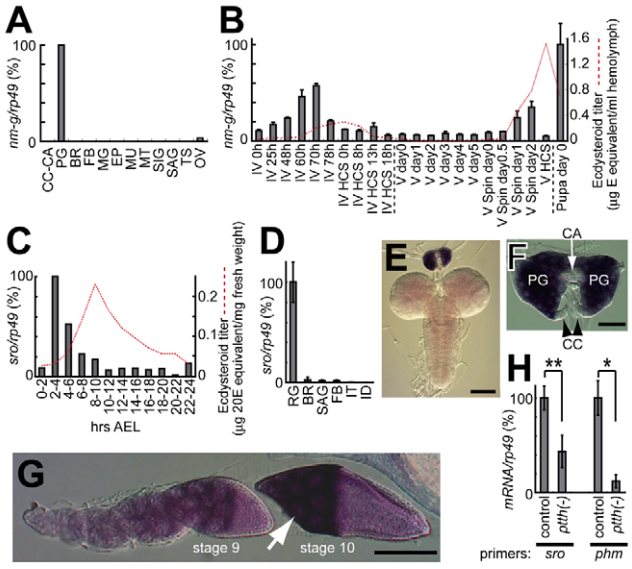

Fig. 5. The expression pattern of *B. mori nm-g* and *D. melanogaster sro*. (**A**) qRT-PCR analysis of the *nm-g* transcript in several tissues from the fifth instar larvae 2 days after the onset of spinning (V spin 2), when the ecdysteroid titer increases (see B). CC-CA, corpus allatum-corpus cardiacum complex; PG, prothoracic gland; BR, brain; FB, fat body; MG, midgut; EP, epidermis; MU, muscle; MT, Malpighian tubules; SIG, silk gland; SAG, salivary gland; TS, testis; OV, ovary. (**B**) The temporal expression profile of *nm-g* in the PG during the fourth larval (IV), fifth larval (V) and pupal stages. Stage of *B. mori* is defined as hours after ecdysis and hours after head capsule slippage (HCS) for the fourth instar larvae, and days after ecdysis, days after spinning (Spin) and the HCS stage for the fifth instar larvae. Under our experimental conditions, the HCSs in the fourth and fifth instar larvae occurred at IV 84 hours and V Spin day 3, respectively. V Spin day 0.5 larvae displayed gut purge. The red line is a schematic representation of developmental changes in hemolymph ecdysteroid titer based on the data as previously described (Kiguchi and Agui, 1981; Kiguchi et al., 1985). Each error bar represents the standard deviation from three independent samples. (**C**) The temporal expression profile of *sro* in *D. melanogaster* embryos. The red line is a schematic representation of the embryonic ecdysteroid titer based on the data as previously described (Maróy et al., 1988). (**D**) The *sro* transcript levels in several larval tissues from wandering third instar larvae of *D. melanogaster*. RG, ring gland; BR, brain; FB, fat body; SAG, salivary gland; IT, intestine; ID, imaginal discs. Each error bar represents the s.e.m. from three independent samples. (**E**,**F**) In situ expression of *sro* in *D. melanogaster*. (E) Brain-ventral nerve cord ring gland complex of the wandering stage of third instar larva. (F) Ring gland of the wandering third instar larva. Arrow and arrowheads indicate the corpus allatum (CA) and the corpus cardiacum (CC), respectively. Scale bars: in E, 100 μm; in F, 25 μm. (**G**) Ovarian expression detected with an antisense probe. Scale bar: 100 μm. (**H**) qRT-PCR analysis of the *sro* and the *phm* transcripts in 120±12 hours AEL third instar larvae of control and *ptth*-expression neuron-ablated [*ptth(–)*] animals. Control animals and *ptth(–)* animals for each individual qRT-PCR experiment were derived from the same progeny of *ptth-GAL4/CyO[gfp];UAS-grim/TM3[gfp]* because the *ptth* neurons are eliminated in homozygotes of both *ptth-GAL4* and *UAS-grim* transgenes (McBrayer et al., 2007). The *phm* transcript was used as a positive control. Each error bar represents the s.e.m. from three independent samples. *, $P<0.05$ and **, $P<0.01$ by paired *t*-test.

A measurement of ecdysteroid titer in *sro* RNAi animals using radioimmunoassay

Because the *B. mori nm-g* mutant larvae are known to exhibit a low ecdysteroid titer (Nagata et al., 1987; Tanaka, 1998), it was expected that the loss of *sro* function would also cause a reduction of the ecdysteroid titer in *D. melanogaster*. We therefore performed a radioimmunoassay to examine whether the *sro* RNAi caused a reduction in ecdysteroid titers. Ethanolic extracts from the control and the *sro* RNAi second instar larvae were prepared 54-66 hours AEL, which is the time when a large amount of 20E is produced in the wild type (Sullivan and Thummel, 2003). However, the *sro* RNAi animals exhibited a normal level of ecdysteroids when compared with the control animals (see Fig. S9 in the supplementary material). This result was in fact consistent with the previous study demonstrating that *sro* mutant embryos do not show the reduced ecdysteroid titer (Chávez et al., 2000). This point is argued in the Discussion below.

nm-g/*sro* plays a crucial role in the Black Box

To determine which ecdysteroid conversion step is affected by the loss of *nm-g*/*sro* function, we performed a feeding experiment with various precursors of ecdysone biosynthesis. We expected that an exogenously applied intermediate downstream of the conversion step by Nm-g/Sro would overcome the larval arrest phenotype observed in the loss of *nm-g*/*sro* function animals. When 5β-ketodiol was added to the food, ~90% of the *B. mori nm-g* mutant animals were rescued and entered the molting stage (Table 2; see Fig. S8 in the supplementary material). Similarly, in *D. melanogaster*, ~70% of the *sro* RNAi animals on 5β-ketodiol-supplemented food molted into the third larval instar (Table 2). By contrast, food containing cholesterol and 7dC did not rescue the

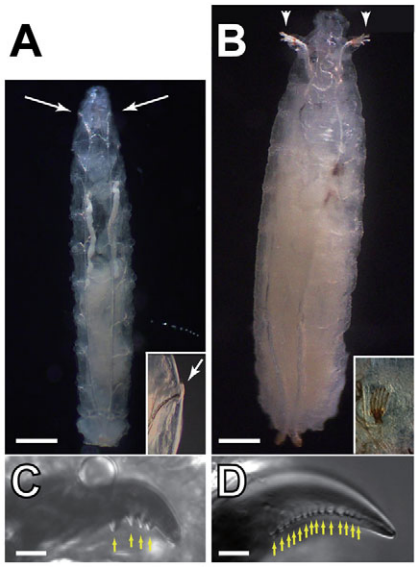

Fig. 6. *D. melanogaster sro* RNAi animals are rescued by the feeding of 5β-ketodiol. (**A-D**) Whole bodies (A,B) and dissected mouth hooks (C,D) of *sro* RNAi animals at 120 hours AEL. The animals were reared on food supplemented with control ethanol (A,C) or 5β-ketodiol (B,D). Yellow arrows indicate the teeth of mouth hooks. *sro* RNAi animals raised on a regular diet died in the second instar larval stage, exhibiting singular insertions of anterior tracheal pits (A, arrows and inset) and 2-5 teeth on mouth hooks (C). 5β-ketodiol-fed *sro* RNAi animals molted in the third instar larval stage as judged by the branched morphology of the anterior tracheal pits (B, arrowheads and inset) and numerous small teeth on the mouth hook (D), which are typical features of third instar larvae. Scale bars: 500 μm in A,B; 10 μm in C,D.

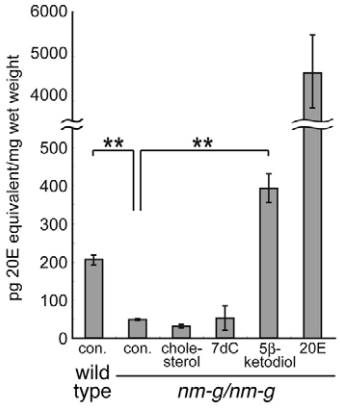

Fig. 7. Ecdysteroid titers in the *B. mori* wild type and the *nm-g* mutants on food supplemented with intermediates. Day 3 wild-type and day 6 *nm-g* mutant first instar larvae were collected and squashed for their measurements (also see Materials and methods). The results are depicted as picograms (pg) of 20E equivalents/mg wet body weight on the *y*-axis. Each bar represents the mean ± s.e.m. from two independent samples for each feeding condition. Control animals (con.) were reared without intermediates. **, $P<0.01$ by Student's *t*-test.

larval growth arrest in the loss of *nm-g*/*sro* function larvae of both species (Table 2; see Fig. S8B,C in the supplementary material). In *B. mori nm-g* mutants, the application of 5β-ketodiol, but not cholesterol or 7dC, also rescued the low ecdysteroid titer and exhibited a higher titer than the wild-type ecdysteroid level (Fig. 7). The failure of feeding rescue by 7dC was not due to the instability and accidental degradation of 7dC under our experimental conditions because the larval growth arrest of *D. melanogaster nvd* RNAi animals (Yoshiyama et al., 2006) was rescued by 7dC from the same reagent stock (93%; n=46). These results suggest that the Nm-g/Sro proteins act upstream of the 5β-ketodiol and downstream of the 7dC production, i.e. in the Black Box in the ecdysteroid biosynthesis pathway (Fig. 1).

Table 2. Rescue experiments with ecdysteroid intermediates

	% of rescued *nm-g*	% of rescued *sro* RNAi
EtOH (control)	0 (30)	0 (71)
Cholesterol	0 (30)	0 (107)
7-dehydrocholesterol	0 (30)	0 (89)
5β-ketodiol	90 (30)	74 (147)
Ecdysone	93 (30)	n.d.
20-hydroxyecdysone	n.d.	43 (118)

The percentage of *nm-g* silkworms that entered into the moulting stage and *sro* RNAi flies growing into the third instar stage was examined. Each number in parentheses refers to the total number of animals in each experiment. n.d., not determined.

DISCUSSION

In this study we identified the *non-molting glossy* (*nm-g*)/*shroud* (*sro*) genes that belong to a family of short-chain dehydrogenase/reductase (SDR) proteins. Some SDRs are involved in steroid biosynthesis in vertebrates (Wu et al., 2007). Although the 3-dehydroecdysone 3α-reductase, which contributes to the inactivation of ecdysteroids, belongs to the SDR family in the cotton leafworm *Spodoptera littoralis* (Takeuchi et al., 2000), no SDRs have been identified as ecdysteroidogenic enzymes so far. All of our results indicate that Nm-g/Sro plays a crucial role in ecdysteroid biosynthesis in insects.

A previous study argued that *D. melanogaster sro* and *kay* belong to the same complementation group (Giesen et al., 2003). However, we consider it unlikely that the gene responsible for the *sro* mutation is *kay*/*D-fos* for the following reasons. First, all EMS-induced *sro* mutants are complemented with the validated *kay* mutant, which is also consistent with a recent report (Hudson and Goldstein, 2008). Second, both of the independent EMS-induced *sro* alleles have nonsense mutations that disrupt the catalytic centers of the SDR proteins. Finally, lethality of the EMS-induced *sro* mutant is rescued by transgenes of *D. melanogaster CG12068* and *B. mori nm-g*. We have assumed that the atypical characteristics of the P-element insertion allele sro^{P54} led to the conclusion of a previous study (Giesen et al., 2003) that showed non-complementation with both *sro* and *kay* (Fig. 4D). Because another previous study argues that the sro^{1} mutant has a point mutation in the first exon of *kay* (Hudson and Goldstein, 2008), we also re-examined their finding. We found three synonymous nucleotide substitutions, but not any nonsynonymous changes, in the ORF region in the first exon of *kay* (see Fig. S10 in the supplementary material). Therefore, the sro^{1} mutant chromosome at least does not cause any amino acid changes in Kay proteins.

B. mori nm-g mutants show a lower ecdysteroid titer during their larval development (Nagata et al., 1987) (Fig. 7). Conversely, radioimmunoassays performed by this study and the previous study (Chávez et al., 2000) demonstrate that *sro* RNAi animals exhibit the normal ecdysteroid titer in *D. melanogaster*. We also measured

the ecdysteroid titer in *sro* RNAi animals supplemented with cholesterol, 7dC, 5β-ketodiol and 20E, but no obvious difference was detected between the control and the *sro* RNAi animals (see Fig. S9 in the supplementary material). The *sro* mutants have been classified as Halloween mutants, many of which exhibit ecdysteroid deficiencies in embryos (Chávez et al., 2000). In addition, the phenotypes caused by the loss of *sro* function are clearly rescued by the application of 20E or 5β-ketodiol, suggesting that *D. melanogaster sro* is essential for ecdysone production as well as *B. mori nm-g*. We assume that the loss of *sro* function might lead to the accumulation of the substrate of Sro in the Black Box. The accumulated substrate might cause a production of an unknown byproduct that can be recognized by an anti-ecdysone antibody used for the radioimmunoassay, as discussed previously (Chávez et al., 2000). The data also suggest an unknown difference in the synthesis and/or metabolism of ecdysteroids between *B. mori* and *D. melanogaster*.

Like the Halloween P450 genes, the spatiotemporal expression pattern of *nm-g*/*sro* correlates with in vivo ecdysone production. Conversely, there are also some differences between *sro* and other Halloween genes. For example, *sro* is not expressed in the primordial PG in the late embryonic stage of *D. melanogaster* (see Fig. S7G in the supplementary material). The embryonic PG is thought to be less crucial for the production of embryonic ecdysteroid, as the ecdysteroid titers continuously and gradually decrease after the primordial ring gland forms by stage 14-15 during embryogenesis (Fig. 5C). Therefore, the embryonic PG without *sro* expression would not affect embryonic ecdysone production. Meanwhile, the difference in expression between *sro* and other Halloween genes suggests that the transcriptional regulation of *nm-g*/*sro* is possibly different from that of the other Halloween genes. The other difference is that the *sro* transcript is not observed in the follicle cells, which are thought to be a source of ecdysone (Riddiford, 1993; Gilbert et al., 2002), but it is seen in the nurse cells (Fig. 5G). Previous studies have shown that all the Halloween genes are expressed mainly in the follicle cells (Chávez et al., 2000; Warren et al., 2002; Petryk et al., 2003; Niwa et al., 2004; Warren et al., 2004; Namiki et al., 2005; Ono et al., 2006). However, it should be noted that another ecdysteroidogenic gene, *neverland*, is strongly expressed in nurse cells (Yoshiyama et al., 2006). In conjunction with our observation, an interesting possibility is that some conversion steps in ecdysteroid biosynthesis take place in the nurse cells and the other steps occur in the follicle cells. If this scenario is correct, certain intermediates should be shuttled between the nurse cells and the follicle cells. Further analysis is needed for understanding of ovarian ecdysteroid production.

The SDR family has great intra- and interspecies functional diversity (Kallberg et al., 2002; Kavanagh et al., 2008). Some mammalian SDRs catalyze the oxidoreduction of hydroxyl and oxo functions at distinct positions in the steroid hormones (Wu et al., 2007), raising the possibility that the Nm-g/Sro proteins could catalyze oxidation or reduction reactions in ecdysteroid biosynthesis. In addition to Halloween P450 Spook and its closest orthologs (Ono et al., 2006), our data suggest that Nm-g/Sro is involved in conversion of 7dC to 5β-ketodiol, the so-called Black Box (Fig. 1), which is considered the rate-limiting step in ecdysteroid biosynthesis (Gilbert et al., 2002). Because overexpression of *nm-g* and *sro* does not affect development, the transcriptional regulation of *nm-g*/*sro* might not be rate-limiting. Thus far, we have not assigned a specific enzymatic activity to any substrate for Nm-g/Sro, as no intermediates between 7dC and 5β-ketodiol have been precisely identified in insects (Warren and Hetru, 1990; Gilbert et al., 2002). One possibility is that Nm-g/Sro catalyzes the 3β-dehydrogenation of 7dC to 3-oxo-7dC (cholesta-5,7-diene-3-one), which is hypothesized to be involved in the initial step in the Black Box (Dauphin-Villemant et al., 1997; Warren et al., 2009). An alternative possibility is that Nm-g/Sro might act as an ecdysteroid 5β-reductase converting Δ^4-diketol to diketol. This is the putative last step in the Black Box proposed from studies using the Y-organ of the crab *Carcinus maenas* (Blais et al., 1996), although Δ^4-diketol has neither been isolated nor shown to be a product in the ecdysteroid biosynthesis pathway in insects (Gilbert et al., 2002). Further studies to identify the exact step in which Nm-g/Sro is involved would shed light on the molecular mechanisms controlling developmental timing in insects. Studies on the elucidation of the enzymatic function of Nm-g/Sro are now underway.

Acknowledgements

We are grateful to Dirk Bohmann, Christian Klämbt, Kazuei Mita, Michael B. O'Connor, Hajime Ono, William M. Saxton, Ben-Zion Shilo, Carl S. Thummel, the *Drosophila* Genetic Resource Center and the Vienna *Drosophila* RNAi Center for stocks and reagents; and Katherine Olsson Carter, Damien Hall and DeMar Taylor for their helpful comments to improve our manuscript. We also deeply thank Yoshihiro Shiraiwa, Katsuo Furukubo-Tokunaga and their laboratory members for allowing R.N. and Y.S.-N. to use their space and equipment. Y.S.-N. and Sh.K. were recipients of fellowships from the Japan Society for the Promotion of Science. This work was supported in part by Special Coordination Funds for Promoting Science and Technology from the Ministry of Education, Culture, Sports, Science, and Technology of the Japanese Government (MEXT) and by the National Bio-Resource Project 'Silkworm' of MEXT. This work was also supported by grants to R.N. from the Inamori foundation; to To.S. and Su.K. from MEXT (No. 17018007, No. 19688004 and the Professional Program for Agricultural Bioinformatics) and MAFF-NIAS (the Agrigenome Research Program); and to Te.S. from the Program for the Promotion of Basic Research Activities for Innovative Biosciences. This article is freely accessible online from the date of publication.

Competing interests statement

The authors declare no competing financial interests.

Supplementary material

Supplementary material for this article is available at
http://dev.biologists.org/lookup/suppl/doi:10.1242/dev.045641/-/DC1

References

Blais, C., Dauphin-Villemant, C., Kovganko, N., Girault, J. P., Descoins, C., Jr and Lafont, R. (1996). Evidence for the involvement of 3-oxo-delta4 intermediates in ecdysteroid biosynthesis. *Biochem. J.* **320**, 413-419.

Brand, A. H. and Perrimon, N. (1993). Targeted gene expression as a means of altering cell fates and generating dominant phenotypes. *Development* **118**, 401-415.

Chávez, V. M., Marques, G., Delbecque, J. P., Kobayashi, K., Hollingsworth, M., Burr, J., Natzle, J. E. and O'Connor, M. B. (2000). The *Drosophila disembodied* gene controls late embryonic morphogenesis and codes for a cytochrome P450 enzyme that regulates embryonic ecdysone levels. *Development* **127**, 4115-4126.

Dauphin-Villemant, C., Bocking, D., Blais, C., Toullec, J. Y. and Lafont, R. (1997). Involvement of a 3beta-hydroxysteroid dehydrogenase activity in ecdysteroid biosynthesis. *Mol. Cell. Endocrinol.* **128**, 139-149.

Ghanim, M. and White, K. P. (2006). Genotyping method to screen individual *Drosophila* embryos prior to RNA extraction. *BioTechniques* **41**, 414-418.

Giesen, K., Lammel, U., Langehans, D., Krukkert, K., Bunse, I. and Klämbt, C. (2003). Regulation of glial cell number and differentiation by ecdysone and Fos signaling. *Mech. Dev.* **120**, 401-413.

Gilbert, L. I. and Warren, J. T. (2005). A molecular genetic approach to the biosynthesis of the insect steroid molting hormone. *Vitam. Horm.* **73**, 31-57.

Gilbert, L. I., Rybczynski, R. and Warren, J. T. (2002). Control and biochemical nature of the ecdysteroidogenic pathway. *Annu. Rev. Entomol.* **47**, 883-916.

Hudson, S. G. and Goldstein, E. S. (2008). The gene structure of the *Drosophila melanogaster* proto-oncogene, kayak, and its nested gene, fos-intronic gene. *Gene* **420**, 76-81.

Ito, K., Kidokoro, K., Sezutsu, H., Nohata, J., Yamamoto, K., Kobayashi, I., Uchino, K., Kalyebi, A., Eguchi, R., Hara, W. et al. (2008). Deletion of a gene

encoding an amino acid transporter in the midgut membrane causes resistance to a *Bombyx* parvo-like virus. *Proc. Natl. Acad. Sci. USA* **105**, 7523-7527.
Ito, K., Katsuma, S., Yamamoto, K., Kadono-Okuda, K., Mita, K. and Shimada, T. (2009). A 25 bp-long insertional mutation in the *BmVarp* gene causes the waxy translucent skin of the silkworm, *Bombyx mori*. *Insect Biochem. Mol. Biol.* **39**, 287-293.
Jürgens, G., Wieschaus, E., Nüsslein-Volhard, C. and Kluding, H. (1984). Mutations affecting the pattern of the larval cuticle in *Drosophila melanogaster* II. Zygotic loci on the 3rd chromosome. *Roux's Arch. Dev. Biol.* **193**, 283-295.
Kallberg, Y., Oppermann, U., Jörnvall, H. and Persson, B. (2002). Short-chain dehydrogenase/reductases (SDRs): Coenzyme-based functional assignments in completed genomes. *Eur. J. Biochem.* **269**, 4409-4417.
Kavanagh, K. L., Jornvall, H., Persson, B. and Oppermann, U. (2008). Medium- and short-chain dehydrogenase/reductase gene and protein families: the SDR superfamily: functional and structural diversity within a family of metabolic and regulatory enzymes. *Cell. Mol. Life Sci.* **65**, 3895-3906.
Kennerdell, J. R. and Carthew, R. W. (2000). Heritable gene silencing in *Drosophila* using double-stranded RNA. *Nat. Biotechnol.* **18**, 896-898.
Kiguchi, K. and Agui, N. (1981). Ecdysteroid levels and developmental events during larval moulting in the silkworm, *Bombyx mori*. *J. Insect Physiol.* **27**, 805-812.
Kiguchi, K., Agui, N., Kawasaki, H. and Kobayashi, H. (1985). Developmental timetable for the last larval and pharate pupal stages in the silkworm, *Bombyx mori*, with special reference to the correlation between the developmental events and haemolymph ecdysteroid levels. *Bull. Sericul. Exp. Stn.* **30**, 83-100.
Lafont, R., Dauphin-Villemant, C., Warren, J. T. and Rees, H. (2005). Ecdysteroid chemistry and biochemistry. In *Comprehensive Molecular Insect Science*, vol. 3 (ed. L. I. Gilbert, K. Iatrou and S. Gill), pp. 125-195. Oxford: Elsevier.
Maróy, P., Kaufmann, G. and Dübendorfer, A. (1988). Embryonic ecdysteroids of *Drosophila melanogaster*. *J. Insect Physiol.* **34**, 633-637.
McBrayer, Z., Ono, H., Shimell, M., Parvy, J. P., Beckstead, R. B., Warren, J. T., Thummel, C. S., Dauphin-Villemant, C., Gilbert, L. I. and O'Connor, M. B. (2007). Prothoracicotropic hormone regulates developmental timing and body size in *Drosophila*. *Dev. Cell* **13**, 857-871.
Mirth, C. K. and Riddiford, L. M. (2007). Size assessment and growth control: how adult size is determined in insects. *BioEssays* **29**, 344-355.
Mita, K., Kasahara, M., Sasaki, S., Nagayasu, Y., Yamada, T., Kanamori, H., Namiki, N., Kitagawa, M., Yamashita, H., Yasukochi, Y. et al. (2004). The genome sequence of silkworm, *Bombyx mori*. *DNA Res.* **11**, 27-35.
Nagata, M., Tsuchida, K., Shimizu, K. and Yoshitake, N. (1987). Physiological aspects of *nm-g* mutant: An ecdysteroid-deficient mutant of the silkworm, *Bombyx mori*. *J. Insect Physiol.* **33**, 723-727.
Namiki, T., Niwa, R., Sakudoh, T., Shirai, K., Takeuchi, H. and Kataoka, H. (2005). Cytochrome P450 CYP307A1/Spook: a regulator for ecdysone synthesis in insects. *Biochem. Biophys. Res. Comm.* **337**, 367-374.
Niwa, R., Matsuda, T., Yoshiyama, T., Namiki, T., Mita, K., Fujimoto, Y. and Kataoka, H. (2004). CYP306A1, a cytochrome P450 enzyme, is essential for ecdysteroid biosynthesis in the prothoracic glands of *Bombyx* and *Drosophila*. *J. Biol. Chem.* **279**, 35942-35949.
Niwa, R., Sakudoh, T., Namiki, T., Saida, K., Fujimoto, Y. and Kataoka, H. (2005). The ecdysteroidogenic P450 *Cyp302a1/disembodied* from the silkworm, *Bombyx mori*, is transcriptionally regulated by prothoracicotropic hormone. *Insect Mol. Biol.* **14**, 563-571.
Ono, H., Rewitz, K. F., Shinoda, T., Itoyama, K., Petryk, A., Rybczynski, R., Jarcho, M., Warren, J. T., Marques, G., Shimell, M. J. et al. (2006). *Spook* and *Spookier* code for stage-specific components of the ecdysone biosynthetic pathway in Diptera. *Dev. Biol.* **298**, 555-570.
Petryk, A., Warren, J. T., Marques, G., Jarcho, M. P., Gilbert, L. I., Kahler, J., Parvy, J. P., Li, Y., Dauphin-Villemant, C. and O'Connor, M. B. (2003). Shade is the *Drosophila* P450 enzyme that mediates the hydroxylation of ecdysone to the steroid insect molting hormone 20-hydroxyecdysone. *Proc. Natl. Acad. Sci. USA* **100**, 13773-13778.
Rewitz, K. F. and Gilbert, L. I. (2008). *Daphnia* Halloween genes that encode cytochrome P450s mediating the synthesis of the arthropod molting hormone: evolutionary implications. *BMC Evol. Biol.* **8**, 60.
Rewitz, K. F., Larsen, M. R., Lobner-Olesen, A., Rybczynski, R., O'Connor, M. B. and Gilbert, L. I. (2009). A phosphoproteomics approach to elucidate neuropeptide signal transduction controlling insect metamorphosis. *Insect Biochem. Mol. Biol.* **39**, 475-483.
Riddiford, L. M. (1993). Hormones and *Drosophila* development. In *The Development of Drosophila melanogaster* (ed. M. Bate and A. Martinez-Arias), pp. 899-939. Cold Spring Harbor, NY: Cold Spring Harbor Laboratory Press.
Shinoda, T. and Itoyama, K. (2003). Juvenile hormone acid methyltransferase: A key regulatory enzyme for insect metamorphosis. *Proc. Natl. Acad. Sci. USA* **100**, 11986-11991.
Spindler, K. D., Honl, C., Tremmel, C., Braun, S., Ruff, H. and Spindler-Barth, M. (2009). Ecdysteroid hormone action. *Cell. Mol. Life Sci.* **66**, 3837-3850.
Sullivan, A. A. and Thummel, C. S. (2003). Temporal profiles of nuclear receptor gene expression reveal coordinate transcriptional responses during *Drosophila* development. *Mol. Endocrinol.* **17**, 2125-2137.
Takeda, S., Kiuchi, M. and Ueda, S. (1986). Preparation of anti-20-hydroxyecdysone serum and its application for radioimmunoassay of ecdysteroids in silkworm hemolymph. *Bull. Sericul. Exp. Stn.* **30**, 361-374.
Takeuchi, H., Chen, J. H., O'Reilly, D. R., Rees, H. H. and Turner, P. C. (2000). Regulation of ecdysteroid signalling: molecular cloning, characterization and expression of 3-dehydroecdysone 3alpha-reductase, a novel eukaryotic member of the short-chain dehydrogenases/reductases superfamily from the cotton leafworm, *Spodoptera littoralis*. *Biochem. J.* **349**, 239-245.
Tanaka, Y. (1998). Induction of larval ecdysis by ecdysone in the *non-molting glossy* (*nm-g*) mutant larvae of *Bombyx mori*. *J. Seric. Sci. Jpn.* **67**, 109-115.
Thompson, J. D., Higgins, D. G. and Gibson, T. J. (1994). CLUSTAL W: improving the sensitivity of progressive multiple sequence alignment through sequence weighting, position-specific gap penalties and weight matrix choice. *Nucleic Acids Res.* **22**, 4673-4680.
Thummel, C. S. (2001). Molecular mechanisms of developmental timing in *C. elegans* and *Drosophila*. *Dev. Cell* **1**, 453-465.
Timmons, L., Becker, J., Barthmaier, P., Fyrberg, C., Shearn, A. and Fyrberg, E. (1997). Green fluorescent protein/β-galactosidase double reporters for visualizing *Drosophila* gene expression patterns. *Dev. Genet.* **20**, 338-347.
Warren, J. T. and Hetru, C. (1990). Ecdysone biosynthesis-pathways, enzymes, and the early steps problem. *Invertebr. Reprod. Dev.* **18**, 91-99.
Warren, J. T., Petryk, A., Marques, G., Jarcho, M., Parvy, J. P., Dauphin-Villemant, C., O'Connor, M. B. and Gilbert, L. I. (2002). Molecular and biochemical characterization of two P450 enzymes in the ecdysteroidogenic pathway of *Drosophila melanogaster*. *Proc. Natl. Acad. Sci. USA* **99**, 11043-11048.
Warren, J. T., Petryk, A., Marques, G., Parvy, J. P., Shinoda, T., Itoyama, K., Kobayashi, J., Jarcho, M., Li, Y., O'Connor, M. B. et al. (2004). *Phantom* encodes the 25-hydroxylase of *Drosophila melanogaster* and *Bombyx mori*: a P450 enzyme critical in ecdysone biosynthesis. *Insect Biochem. Mol. Biol.* **34**, 991-1010.
Warren, J. T., O'Connor, M. B. and Gilbert, L. I. (2009). Studies on the black box: Incorporation of 3-oxo-7-dehydrocholesterol into ecdysteroid by *Drosophila melanogaster* and *Manduca sexta*. *Insect Biochem. Mol. Biol.* **39**, 677-687.
Wu, X., Lukacik, P., Kavanagh, K. L. and Oppermann, U. (2007). SDR-type human hydroxysteroid dehydrogenases involved in steroid hormone activation. *Mol. Cell. Endocrinol.* **265-266**, 71-76.
Xia, Q. Y., Wang, J., Zhou, Z. Y., Li, R. Q., Fan, W., Cheng, D. J., Cheng, T. C., Qin, J. J., Duan, J., Xu, H. F. et al. (2008). The genome of a lepidopteran model insect, the silkworm *Bombyx mori*. *Insect Biochem. Mol. Biol.* **38**, 1036-1045.
Yamamoto, K., Narukawa, J., Kadono-Okuda, K., Nohata, J., Sasanuma, M., Suetsugu, Y., Banno, Y., Fujii, H., Goldsmith, M. R. and Mita, K. (2006). Construction of a single nucleotide polymorphism linkage map for the silkworm, *Bombyx mori*, based on bacterial artificial chromosome end sequences. *Genetics* **173**, 151-161.
Yamamoto, K., Nohata, J., Kadono-Okuda, K., Narukawa, J., Sasanuma, M., Sasanuma, S., Minami, H., Shimomura, M., Suetsugu, Y., Banno, Y. et al. (2008). A BAC-based integrated linkage map of the silkworm *Bombyx mori*. *Genome Biol.* **9**, R21.
Yoshiyama, T., Namiki, T., Mita, K., Kataoka, H. and Niwa, R. (2006). Neverland is an evolutionally conserved Rieske-domain protein that is essential for ecdysone synthesis and insect growth. *Development* **133**, 2565-2574.
Zeitlinger, J., Kockel, L., Peverali, F. A., Jackson, D. B., Mlodzik, M. and Bohmann, D. (1997). Defective dorsal closure and loss of epidermal *decapentaplegic* expression in *Drosophila fos* mutants. *EMBO J.* **16**, 7393-7401.